Article

Single-Step Preparation of Mesoporous, Anatase-Based Titanium–Vanadium Oxide and Its Application

Jing-Jong Shyue, and Mark R. De Guire

J. Am. Chem. Soc., **2005**, 127 (36), 12736-12742• DOI: 10.1021/ja0536365 • Publication Date (Web): 20 August 2005

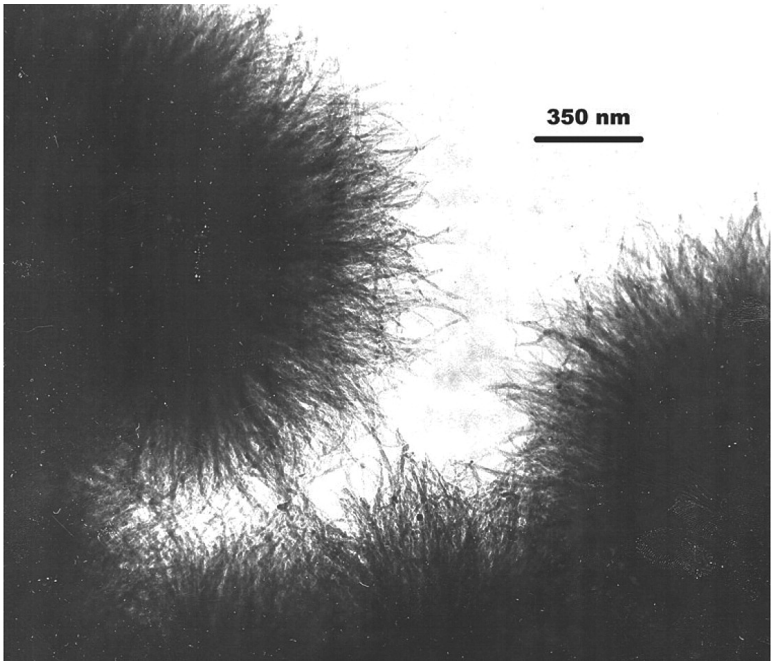

J|A|C|S
ARTICLES
Published on Web 08/20/2005

Single-Step Preparation of Mesoporous, Anatase-Based Titanium−Vanadium Oxide and Its Application

Jing-Jong Shyue† and Mark R. De Guire*

Contribution from the Department of Materials Science & Engineering, Case Western Reserve University, 10900 Euclid Avenue, Cleveland, Ohio 44106-7204

Received June 2, 2005; E-mail: mrd2@case.edu

Abstract: Mesoporous solid solutions of anatase-based titanium−vanadium oxides were synthesized from aqueous solutions. The V/Ti ratio was determined by the composition of the deposition solution, while the morphology and nanoscale porosity were controlled using micelles of the surfactants cetyltrimethylammonium bromide (CTAB), or hexadecylamine (HDA). The use of CTAB resulted in mesoporous powders, whereas HDA yielded clusters of nanotubes. As compared to materials of the same composition made without the use of a surfactant, the catalyst made with CTAB had 50% higher catalytic activity, and that made with HDA had 70% higher activity. As compared to titania-supported vanadia catalysts with equivalent vanadium loading and synthesized using wet impregnation, the co-deposited materials exhibited significantly higher (up to 3.8×) catalytic activity.

Introduction

The major nonmetallurgical use of vanadium is in catalysis. In a recent review of the literature from 1967 to 2000 on transition metal oxide catalysts, 28% of the papers are on vanadium oxides and 15% are on titanium oxides.[1] Therefore, the synthesis of mixed titanium−vanadium oxides may be of interest for potential heterogeneous catalysts. Although most vanadium-based catalysts consist of a vanadium oxide phase deposited on the surface of an oxide support (prepared separately), mixed titanium−vanadium oxide thin films can be co-deposited from aqueous solutions on organic self-assembled monolayers in a single step.[2]

With heterogeneous catalysts, for the same loading of the active component(s), the rate of reaction is a function of the available surface area. Therefore, porous supports are usually used, for example, high-area silica or γ-alumina. The greater is the amount of surface that is accessible to reactants, the larger is the amount of reactant converted to product per unit time per unit catalyst mass. For many applications, a mesoporous structure (2−50 nm) provides a significantly high surface area while providing passages wide enough for the ingress of reactants and egress of products.

The chemical diversity achieved in ordered composite mesoporous materials has expanded during the past decade.[3−19] The general synthetic approach makes use of the micelles formed by surface-active agents (surfactants), molecules with a polar hydrophilic head and a hydrophobic tail (often an alkyl chain). If surfactants are added to water, the hydrocarbon chains tend to self-assemble to minimize their contact with water, causing them to aggregate in various forms such as spheres, rods, and bundles of rods.[20] This approach has been applied to the synthesis of a variety of ceramics, including MCM-41 (silica) and metal phosphates.[21]

Nesper et al. used this approach to synthesize mixed-valence vanadium oxide nanotubes.[22] Protonated primary alkylamines serve both as templates on which the vanadium oxide forms and as spacers between adjacent layers in the walls of the multiwalled nanotubes. This shows that vanadium oxide-based materials with high surface area can be synthesized by using surfactants as templates. The present work seeks a synthesis route that yields a mesoporous vanadium oxide catalyst and support in a single synthesis step from an aqueous solution.

† Current address: Department of Materials Science & Engineering, The Ohio State University, 2041 College Road, Columbus, OH 43210.

(1) Weckhuysen, B. M.; Keller, D. E. *Catal. Today* **2003**, *78*, 25−46.
(2) Shyue, J.-J.; De Guire, M. R. *Trans. Mater. Res. Soc. Jpn.* **2004**, *29*, 2383−2386.
(3) Tiemann, M.; Froba, M. *Chem. Mater.* **2001**, *13*, 3211−3217.
(4) Kresge, C. T.; Leonowicz, M. E.; Roth, W. J.; Varuli, J. C.; Beck, J. S. *Nature* **1992**, *359*, 710−712.
(5) Huo, Q. *Nature* **1994**, *368*, 317−321.
(6) Tanev, P. T.; Pinnavaia, T. J. A. *Science* **1995**, *267*, 865−867.
(7) Antonelli, D. M.; Ying, J. Y. *Angew. Chem., Int. Ed. Engl.* **1996**, *35*, 426−430.
(8) Attrad, G. S. *Science* **1997**, *278*, 838−840.
(9) Zhao, D. *Science* **1998**, *279*, 548−552.
(10) Yang, P.; Zhao, D.; Margolese, D. I.; Chemelka, B. F.; Stucky, G. D. *Nature* **1998**, *396*, 452−155.
(11) Asefa, T.; MacLachlan, M. J.; Coombs, N.; Ozin, G. A. *Nature* **1999**, *402*, 867−871.
(12) Ryoo, R.; Joo, S. H.; Jun, S. *J. Phys. Chem.* **1999**, *103*, 7743−7749.
(13) Inagaki, S.; Guan, S.; Ohsuna, T.; Terasaki, O. *Nature* **2002**, *416*, 304−307.
(14) Schuth, F. *Chem. Mater.* **2001**, *13*, 3184−3195.
(15) Sakamoto, Y. *Nature* **2000**, *408*, 449−453.
(16) Stucky, G. D. *Stud. Surf. Sci. Catal.* **1997**, *105*, 3−28.
(17) Corriu, R. J. P.; Leclercq, D. *Angew. Chem., Int. Ed. Engl.* **1996**, *35*, 1420−1436.
(18) Vioux, A. *Chem. Mater.* **1997**, *9*, 2292−2299.
(19) Ying, J. Y.; Mehnert, C. P.; Wong, M. S. *Angew. Chem., Int. Ed.* **1999**, *38*, 56−77.
(20) Evans, D. F.; Mitchell, D. G.; Ninham, B. W. *J. Phys. Chem.* **1986**, *90*, 2817−2825.
(21) Tian, B.; Liu, X.; Tu, B.; Yu, C.; Fan, J.; Wang, L.; Xie, S.; Stucky, G. D.; Zhao, D. *Nat. Mater.* **2003**, *2*, 159−163.
(22) Muhr, H.-J.; Krumeich, F.; Schönholzer, U. P.; Bieri, F.; Niederberger, M.; Gauckler, L. J.; Nesper, R. *Adv. Mater.* **2000**, *12*, 231−234.

10.1021/ja0536365 CCC: $30.25

Table 1. Amounts of Chemicals Used To Prepare Ti−V Oxide Powder[a]

$(NH_4)VO_3$ (g)	0.0585	0.2340	0.1170	0.2925	0.2925	0.3509	0.4678	0.9358
$(NH_4)_2TiF_6$ (g)	1.9797	1.5838	1.5838	1.3858	0.9899	0.9899	0.4949	0.4949
boric acid (g)	1.8549	1.4839	1.4839	1.2984	0.9275	0.9275	0.4637	0.4637
oxalic acid (g)	0.1838	0.3675	0	0	0	0	0	0
[Ti] (mM)	100	80	80	70	50	50	25	25
[V] (mM)	5	20	10	25	25	30	40	80
[oxalic] (mM)	20	40	0	0	0	0	0	0
yield (without surfactant, %)	20.5	21.9	91.1	81.6	65.8	63.0	46.7	40.4
V% in powder (w/o surfactant)	17	35	42	48	55	58	70	79
yield (with CTAB, %)	70.5	54.7	99.1	97.8	94.2	92.8	70.9	85.3
V% in powder (with CTAB)	20	37	42	51	55	58	76	83
yield (with HDA, %)	20.5	21.9	81.1	96.8	85.4	81.6	67.5	58.4
V% in powder (with HDA)	22	37	41	48	55	60	74	82

[a] Compositions were determined by XEDS and are reported in units of cat. %.

The reaction used to evaluate the catalytic activity of the titanium−vanadium oxide materials prepared here was the conversion of (±)-lactic acid to pyruvic acid in an aqueous environment. Pyruvic acid, an important metabolite in all microorganisms and a useful intermediate for drug synthesis, has been synthesized by the fermentation of various hydrocarbons including glucose and peptone.[23] However, these methods produce pyruvic acid with low yield in a mixture of fermentation products. Microbiological oxidation of pure D(−)-lactic acid (a form that is less common in nature) to pyruvic acid has been described,[24] as has conversion of L(+)-lactic acid using glycolate oxidase.[25]

Experimental Procedures

Preparation of Titanium−Vanadium Oxide Powder. The synthesis method was based on a liquid-phase deposition procedure for fabricating TiO_2 coatings.[26] Desired amounts (Table 1) of ammonium metavanadate [$(NH_4)VO_3$] and boric acid (H_3BO_3) were dissolved in 80 mL of distilled water at 80 °C. After the solution cooled to room temperature, desired amounts of oxalic acid [$(COOH)_2$] were added to the low-vanadium solutions. (Oxalic acid preferentially chelated vanadium ions, making it easier to achieve materials with low vanadium content.[27]) The pH was then adjusted to around 2.5 by adding 1 M HCl aqueous solution. Desired amounts of ammonium hexafluorotitanate [$(NH_4)_2TiF_6$] and optional 10 mL of 0.1 M *N*-cetyl-*N*,*N*,*N*-trimethylammonium bromide [CTAB, $C_{16}H_{33}N(CH_3)_3Br$] or 10 mL of 0.01 M *n*-hexadecylamine (HDA, $C_{16}H_{33}NH_2$) aqueous solution were added. The pH was again adjusted to around 2.5 by adding 1 M HCl aqueous solution. The whole solution was then diluted to 100 mL (final surfactant concentrations of 10 mM for CTAB and 1 mM for HDA, 10 times their critical micelle concentration). This solution was used immediately after being prepared.

The deposition solutions were covered and placed in an oil bath at 45 °C for 24 h. The resulting powder was collected using filter paper (medium-fine pore) and washed with 50 mL of distilled water four times and 50 mL of ethanol twice to remove the organic template. (The ethanol rinse also served the purpose of removing some of the adsorbed water.) The powder (yellow to orange-brown, indicative of V^{5+}) was dried under 1 Pa at room temperature overnight. The powder was loosely agglomerated, typical of mesoporous solids such as MCM-41, and was used without further treatment.

Preparation of Reference Catalyst. Titania-supported vanadium oxide with 0, 5, 10, 15, 20, 25, 30, 35, and 40 cat. % V (cation ratio) was prepared using the wet impregnation technique. Titania (Aldrich, 15 nm average diameter, with surface area of 133 m^2/g as measured here, and 190−290 m^2/g specified by the supplier) was dispersed in an aqueous solution of ammonium metavanadate (<100 mM) by stirring. Water was slowly evaporated at 80 °C with continuous stirring to form a slurry. The slurry was dried at 120 °C and calcined in air at 420 °C for 3 h.[28]

Chemical and Structural Characterization of Powders. X-ray energy-dispersive spectroscopy (XEDS) was carried out with a Si(Li) detector made by Noran attached to a Philips XL30 environmental scanning electron microscope (ESEM). An accelerating voltage of 20 kV was used to excite Ti K_α (4.510 keV) and V K_α (4.952 keV) emission. The resulting spectra were quantitatively analyzed using the filter fit method without standards. The X-ray diffraction (XRD) patterns were recorded on a Scintag Advanced Diffraction System with Cu Kα X-ray source.

The specimens for transmission electron microscopy (TEM) were prepared by dropping an ethanol suspension of the powder onto an amorphous carbon foam, supported by a Cu grid. The specimen was allowed to dry under air at room temperature for 10 min.

Conventional TEM images were taken with a Philips CM-20 microscope with a 200 keV electron beam. The objective aperture was used to generate the diffraction contrast. The magnification was calibrated with Pelco grating replicas with 2160 lines/mm.

Nitrogen adsorption−desorption was measured with a Micromeritics FlowSorb II 2300 on catalysts (50−150 mg) with about 50 cat. % surface V loading (10 cat. % in the bulk reference catalyst; 48 cat. % for catalysts deposited without surfactant and with 1 mM HDA; and 51 cat. % for catalysts deposited with 10 mM CTAB). Catalysts were freeze-dried under 200 mTorr at −40 °C for 100 min, slowly heated to 0 °C (450 min ramp), and held at that temperature for 60 min. The samples were then allowed to return to room temperature (20 °C) under 150 mTorr in 30 min. The condenser was at −80 °C during the whole procedure. Before each adsorption−desorption run, the sample was degassed in situ in the system with flowing N_2/He mixture (60 mL/min) for 20 min. Nitrogen (30% N_2 in He, $P/P_0 = 0.3$) was absorbed at liquid nitrogen temperature (77 K) and was desorbed at room

(23) Oneil, M. J.; Smith, A. *The Merck Index on CD-ROM*, 12:1 ed.; Merck & Co., Inc., Chapman & Hall EPD: Whitehouse Station, NJ, 2001.
(24) Brian, C. U.S. Patent No. 4900668, Feb. 13, 1990.
(25) Anton, D. L.; Dicosimo, R.; Witterholt, V. G. U.S. Patent No. 5538875, Jul. 23, 1996.
(26) Kawahara, H.; Honda, H. Japan Pat. No. 59141441A, 1984.
(27) Shyue, J.-J.; De Guire, M. R. *Chem. Mater.*, submitted.
(28) Ciambelli, P.; Bagnasco, G.; Lisi, L.; Turco, M.; Chiarello, G.; Musci, M.; Notaro, M.; Robba, D.; Ghetti, P. *Appl. Catal., B* **1992**, *1*, 61−77.

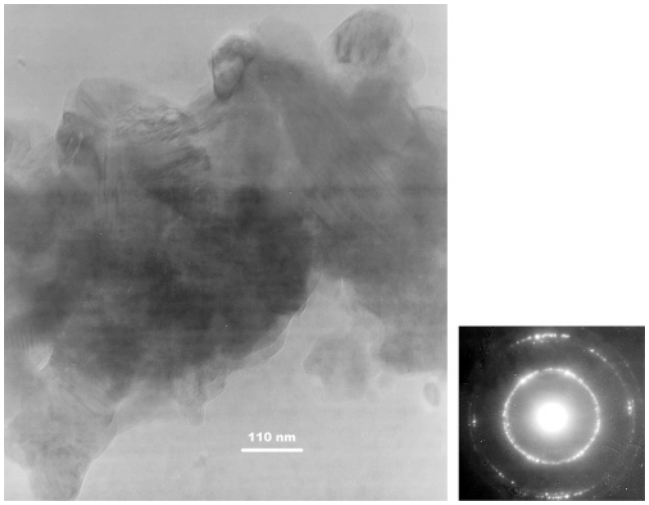

Figure 1. TEM bright-field image of 45 cat. % titanium−55 cat. % vanadium oxide powder prepared from aqueous solution via co-deposition without surfactant.

temperature. The surface areas were calculated from the volume of desorbed nitrogen using the BET formalism[29] and were the average of values from two adsorption−desorption cycles. The catalysts were checked with TEM to confirm that freeze-drying had caused no appreciable alteration of the morphology.

Oxidation of Lactic Acid. Nuclear magnetic resonance (NMR) spectra were used to monitor the reaction. Spectra were reported in units of δ and were recorded on a Varian XL-300 300 MHz spectrometer in D_2O solvent.

20.6 mL 30% H_2O_2 and 8.8 mL 85% lactic acid were dissolved in water and diluted to 1000 mL, yielding a solution with 200 mM H_2O_2 and 100 mM lactic acid. For 100 mL of solution, 5 mg of Ti−V oxide was added. At a given time, the solution was filtered through a nylon membrane with 0.2 μm pores to remove solid catalyst prior to determination of the extent of the intended reaction. The product was purified and identified as hydrated pyruvic acid [^{1}H NMR (300 MHz, D_2O) δ 2.02 (s); ^{13}C NMR (75 MHz, D_2O) δ 20.5, 100.9, 176.8; m/z = 88].

Analysis of Kinetic Constant of Reaction. The reacted solution was analyzed with reverse phase (ODS) HPLC using a UV detector at 210 nm. The mobile phase was distilled water with the flow rate of 4 mL/min. Three peaks could be identified in the HPLC trace at 1.5, 3.5, and 4.8 min, corresponding to H_2O_2, pyruvic acid, and lactic acid, respectively. The concentration of lactic acid left was calculated using [Lactate] = 100 mM × $A_{\text{lactic acid}}/(A_{\text{lactic acid}} + A_{\text{pyruvic acid}})$, where A represents the area of the HPLC peak for the respective species. The concentration as a function of reaction time yields the kinetic constant for the reaction, directly reflecting the activity of the catalyst.

Results and Discussion

Morphologies of Co-deposited Titanium−Vanadium Oxides. Without surfactant, the microstructure of the co-deposited Ti−V oxides was indistinct (Figure 1). The individual particles were about 100 nm in diameter. The electron diffraction pattern showed a polycrystalline anatase structure, which was confirmed by XRD (see below).

In materials synthesized with 10 mM CTAB, long tubular structures hundreds of nanometers long, from 25 nm to at least 70 nm in total width, and exhibiting striations 4 nm wide, were commonly seen (Figure 2). Changing the tilt of such specimens indicated that the striations were not artifacts. Such features are

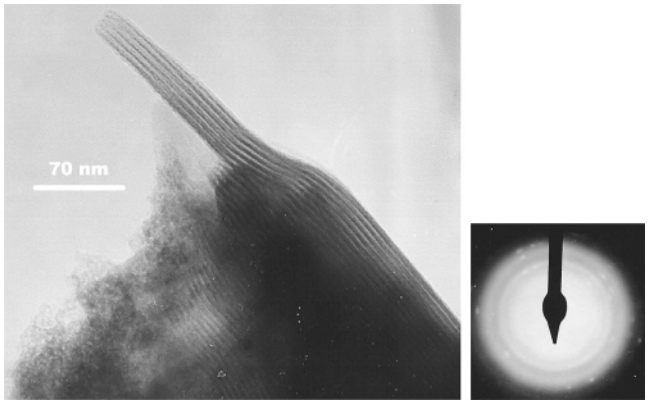

Figure 2. TEM bright-field image of 45 cat. % titanium−55 cat. % vanadium oxide powder prepared from aqueous solution with 10 mM CTAB via co-deposition.

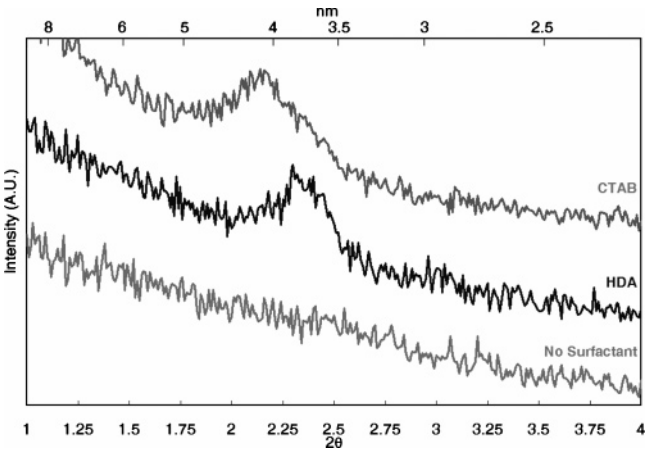

Figure 3. Low-angle XRD traces of Ti−V oxides made with and without surfactant.

typical of known mesoporous materials such as MCM-41 and metal phosphates.[21] We interpret such features to be bundles of parallel tubes, with the dark striations showing the wall thickness (2−6 nm) and the spacing between them showing the tubes' inner diameter (~4 nm). This interpretation is corroborated by low-angle XRD traces that showed diffraction peaks characteristic of features with 4.1 nm periodicity (Figure 3). The diffuse rings of the electron diffraction pattern (Figure 2) show that the material was polycrystalline anatase (confirmed by XRD, see below), but with a finer crystal size than that seen in the material made without using surfactant (Figure 1).

With 1 mM *n*-hexadecylamine (HDA), the microstructure consisted of large clusters that looked like cactuses (Figure 4) with the needles around 10 nm in diameter. The dark centers of the clusters of Figure 4 were too thick for the electron beam to penetrate. However, the centers of smaller clusters consisted of tangled filaments (Figure 5) ranging in diameter from 6 to 10 nm. Low-angle XRD traces showed a diffraction peak at 3.7 nm (Figure 3). If this value represents the minimum periodicity of individual tubes, then the wall thickness can be inferred to be approximately 2 nm, and the thicker filaments could consist of multiple parallel tubes. More detailed TEM characterization was made difficult because recrystallization was observed during prolonged e-beam exposure, and the nanostructure collapsed. Electron diffraction (Figure 4, inset) showed only peaks for polycrystalline anatase (confirmed by XRD, see below).

(29) Brunauer, S.; Emmett, P. H.; Teller, E. *J. Am. Chem. Soc.* **1938**, *60*, 309.

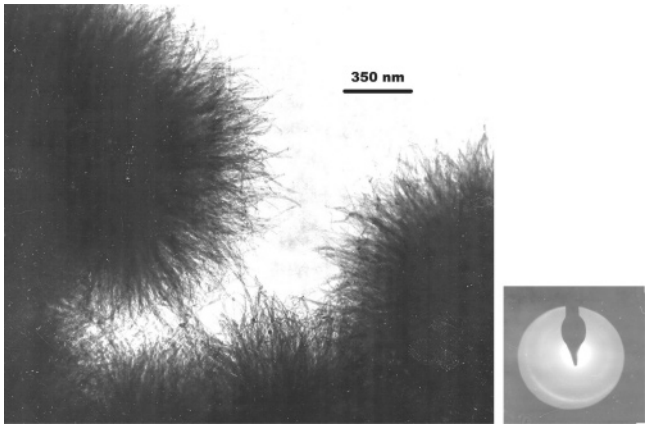

Figure 4. TEM bright-field image of 45 cat. % titanium−55 cat. % vanadium oxide powder made from aqueous solution with 1 mM HDA via co-deposition.

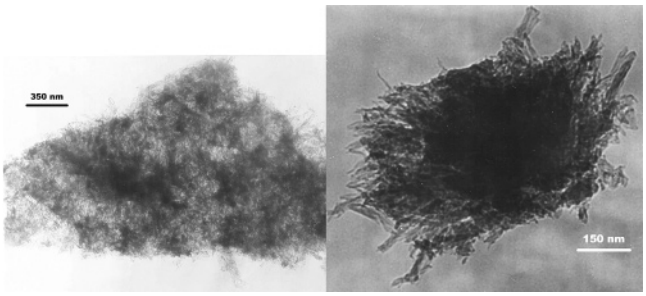

Figure 5. TEM bright-field image of 45 cat. % titanium−55 cat. % vanadium oxide powder (thin particle) made from aqueous solution with 1 mM HDA via co-deposition.

The concentrations of the surfactants used here were both approximately 10× the critical micelle concentrations (CMC), as determined by contact angle measurements at various surfactant concentrations (data not shown here) and by comparison with the literature.[30,31] At lower surfactant concentrations, the evidence of mesoporosity (in the low-angle XRD peaks, Figure 3) was weaker, whereas at higher concentrations, additional weaker low-angle peaks were observed, indicating the appearance of secondary, smaller pores.

The different morphologies produced by the surfactants can be attributed to their different CMCs. Previous work[2] showed that, when no surfactant was used, nanoparticles formed in the solution and attached to each other, forming featureless aggregates. With CTAB at 10 mM, tubular micelles formed; these attracted the species that were present in the solution and self-aligned, yielding a mesoporous structure. The CMC of HDA is an order of magnitude lower (0.1 mM) than that of CTAB. With HDA at 1 mM, the distance between micelles was larger than that with CTAB. As a result, the tubes were farther apart and unaligned, forming tangled clusters on drying.

The surfactants used here range from strongly cationic (CTAB) to weakly basic (HDA) in character. Both succeeded in inducing the formation of the mixed titanium−vanadium oxide on the charged surfaces of the resulting micelles. This outcome was consistent with observations that organic self-assembled monolayers (SAMs) with a similar range of surface functionalities (alkylammonium and amine[32]) promoted the deposition of vanadium oxide films and mixed titanium−vanadium oxide films on silicon substrates.[2,33−35] In both cases (co-deposited powders and films), the result is believed to be due to the negative charge on aqueous vanadium complexes and/or vanadium oxide particle surfaces as opposed to the positive charge of aqueous titanium complexes[36] and titanium oxide particles. In the case of the films (discussed in more detail elsewhere[2,37]), it could not be determined whether the deposits (which were noncrystalline) consisted of agglomerates of nanoscaled but distinct vanadium oxide and titanium particles (which would have experienced mutual attraction from their opposite surface potentials at the pH of deposition) or smaller groupings such as separate vanadium and titanium complexes (which, on the basis of each metal's known aqueous chemistry, would also be expected to be opposite in sign under the deposition conditions) or even mixed vanadium−titanium units. In contrast, the diffraction data from the powders described here indicate the presence of $(Ti,V)O_{2+\delta}$ solid solutions with the anatase structure (see below), with the lattice parameter varying as expected (see below) with the Ti/V ratio in the solids. This suggests that these powders formed via the assembly of ions or complexes rather than particles.

There are significant similarities and differences between the mesoporous materials reported here and the multiwalled, mixed-valence vanadium oxide nanotubes of Nesper et al.[22] The positively charged end of a long-chain hydrocarbon (an alkylammonium or a protonated amine group) appears to play a crucial role in inducing the formation of the oxide phase and in templating its growth as walls of nanotubes in all cases. The nanotubes in Nesper's work were predominantly in the form of scrolls, with inner diameters ranging up to 50 nm, and the length of the hydrocarbon chain dictating the spacing between layers of the scroll. In the present work, the inner diameter of the tubes corresponds roughly to twice the length of the hydrocarbon chain. Last, the present materials were made in a single step at 45 °C and atmospheric pressure, whereas the earlier materials required hydrothermal aging (but with a high yield of nanotubes).

Crystallography of Co-deposited Titanium−Vanadium Oxide. The *d*-spacings of the anatase phase decreased as the vanadium content increased (Figure 6, Table 2). As V^{5+} is smaller[38] than Ti^{4+}, this suggests that the phase was a $(Ti,V)O_{2+\delta}$ substitutional solid solution. Assuming the lattice parameters to vary linearly between those of anatase (tetragonal, $a = 0.3782$ nm, $c = 0.9502$ nm[39]) and $V_2O_5 \cdot 1.6H_2O$ (orthorhombic, $a = 0.356$ nm, $b = 0.437$ nm, $c = 1.155$ nm[40]), the predicted values of d_{101} and d_{200} for each composition agreed with the

(30) Adamson, A. W.; Gast, A. P. *Physical Chemistry of Surfaces*, 6th ed.; John Wiley & Sons: New York, 1997.
(31) Shaw, D. J. *Introduction to Colloid and Surface Chemistry*, 3rd ed.; Butterworth-Heinemann: Boston, 1992; pp 148−162.
(32) Shyue, J.-J.; De Guire, M. R.; Nakanishi, T.; Masuda, Y.; Koumoto, K.; Sukenik, C. N. *Langmuir* **2004**, *20*, 8693−8698.
(33) Shyue, J.-J.; De Guire, M. R. In *CIMTEC 2002 (10th International Ceramics Congress and 3rd Forum on New Materials)*; Vincenzini, P., Ed.; Florence, Italy, 2002; p 469.
(34) Shyue, J.-J.; De Guire, M. R. *Chem. Mater.* **2005**, *17*, 787−794.
(35) Shyue, J.-J.; Tang, Y.; De Guire, M. R. *J. Mater. Chem.* **2005**, *15*, 323−330.
(36) Baes, C. F. J.; Mesmer, R. E. *The Hydrolysis of Cations*; Robert E. Krieger Publishing Co., Inc.: Malabar, FL, 1976; pp 197−210.
(37) Shyue, J.-J. Synthesis of Titanium−Vanadium Oxide Materials from Aqueous Solutions via Co-deposition. Thesis in Department of Materials Science and Engineering; Case Western Reserve University: Cleveland, OH, 2004.
(38) Shannon, R. D. *Acta Crystallogr.* **1976**, *A32*, 751−767.
(39) Joint Committee on Powder Diffraction Standards (JCPDS) 84-1266.
(40) Joint Committee on Powder Diffraction Standards (JCPDS) 40-1296.

Table 2. Expected and Observed Anatase (101) and (200) Interplanar Spacings (nm) in Ti−V Anatase Solid Solutions (cat. %)

	anatase	17%	35%	42%	48%	58%	70%	79%	vanadia
$a_{calc.}$	0.378	0.374	0.370	0.369	0.368	0.365	0.363	0.361	0.356
$c_{calc.}$	0.950	0.984	1.020	1.034	1.046	1.066	1.090	1.108	1.150
$d_{101,calc.}$	0.351	0.350	0.348	0.347	0.347	0.346	0.344	0.343	0.340
$d_{101,obs.}$		0.350	0.349	0.348	0.347	0.346	0.344	0.342	
$d_{200,calc.}$	0.189	0.187	0.185	0.184	0.184	0.183	0.181	0.180	0.340
$d_{200,obs.}$		0.187	0.185	0.184	0.184	0.182	0.181	0.180	

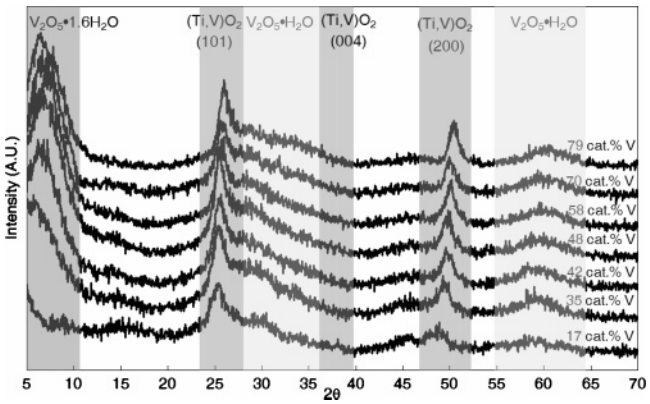

Figure 6. XRD traces of various compositions of Ti−V oxide powders made without surfactant.

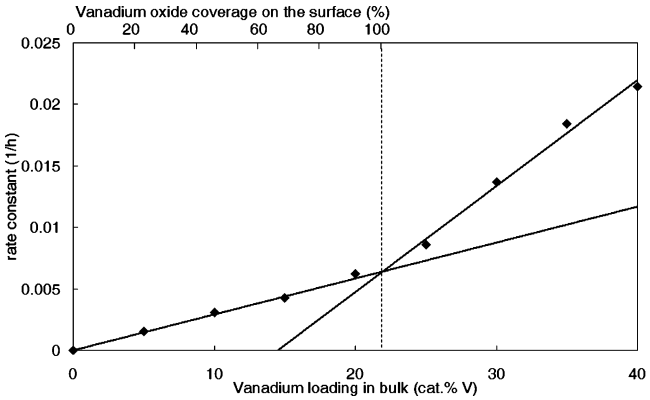

Figure 7. Kinetic constant for reaction 1 versus vanadium loading for reference catalysts.

observed ones to ±1 pm (Table 2). Figure 6 shows also that $V_2O_5 \cdot 1.6H_2O$ and $V_2O_5 \cdot H_2O$ phases were observed.

Oxidation of Lactic Acid. The alcohol group on the α-carbon of lactic acid is a reductive group that can be oxidized to a carbonyl group, while V^{5+} conversely is an oxidative reagent. After exposure of aqueous lactic acid to the mixed titanium−vanadium oxides produced here, the solution's ^{1}H NMR spectrum lacked the peak from the proton on the α-carbon, indicating oxidation of the lactic acid. The GC−MS showed a peak at $m/z = 88$, and the ^{13}C NMR spectrum showed a peak at ∼100 ppm, suggesting that the oxidized product was in the form of the geminal diol instead of carbonyl group (140−180 ppm). Therefore, the observed reaction was[41]

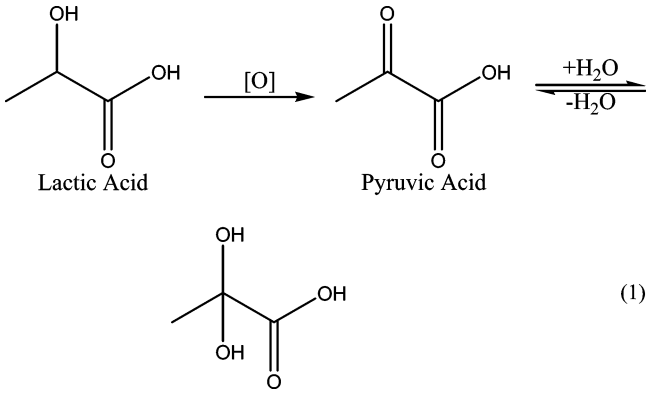

(1)

Catalytic Activity of Anatase-Supported Vanadium Oxides (Reference Catalysts). Titania-supported vanadia catalysts were prepared as reference materials using a conventional wet-impregnation method.[28] The activity of these materials as a function of their vanadium content was assumed to consist of two regimes. At low vanadium contents, the activity was expected to increase linearly with vanadium concentration, as more of the titania surface became covered with the catalytically active vanadium species. In this regime, the effect of the catalyst composition on its surface area was assumed to be negligible.[28] This regime was assumed to extend to the composition at which the titania surface was completely covered with a monolayer of vanadia.[42,43]

At higher vanadium concentrations, two circumstances may occur. In one, the vanadium in excess of a monolayer may form clusters on the surface, blocking pores and decreasing the surface area[44] without increasing the effective vanadium surface concentration beyond 100%. In this case, the activity of the catalyst is expected to decrease with increasing vanadium loading beyond monolayer coverage. Another possibility is that vanadium in excess of a monolayer, that is, vanadium not bonded directly to the titania support, may dissolve in the aqueous environment of the test reaction. If the solvated vanadium species can still catalyze the reaction, an increase in apparent activity might be observed with increasing nominal vanadium content of the catalyst. In either case, a deviation from the submonolayer linear trend would be expected, with the vanadium concentration at which the deviation occurred indicating the composition that corresponds to full monolayer coverage.

Up to ∼20 cat. % V, the kinetic constant for reaction 1 increased linearly with vanadium concentration in the anatase-supported vanadium oxide catalyst (Figure 7). Beyond 20 cat. % V, the slope of the kinetic constant versus vanadium concentration increased abruptly, by a factor of 3. The intersection of the two linear regimes at 21.8% vanadium was taken to be the limit of monolayer coverage for the reference catalysts. Subsequent experiments showed that the increased kinetics of

(41) Grossman, R. B. *The Art of Writing Reasonable Organic Reaction Mechanisms;* Springer-Verlag New York, Inc.: New York, 1999; p 278.

(42) Centi, G.; Giamello, E.; Pijnelli, D.; Trifiro, F. *J. Catal.* **1991**, *130*, 220−237.

(43) Bulushev, D. A.; Kiwi-Minsker, L.; Renken, A. *Catal. Today* **2000**, *57*, 231−239.

(44) Oliveri, G.; Ramis, G.; Busca, G.; Escribano, V. S. *J. Mater. Chem.* **1993**, *3*, 1239−1249.

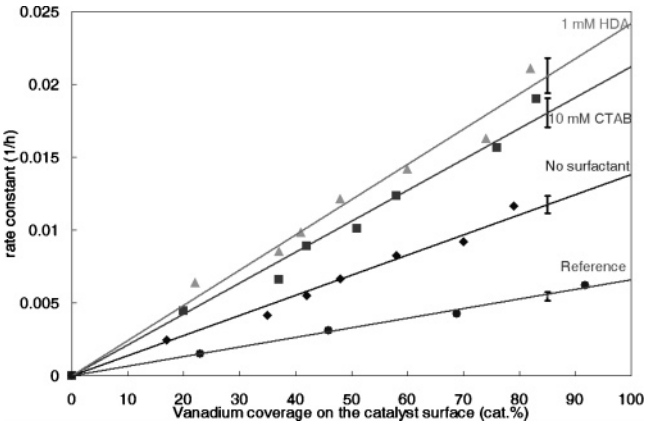

Figure 8. Kinetic constant for reaction 1 versus vanadium loading for co-deposited vanadia−titania catalysts. The error bars show the 95% confidence limit.

Table 3. Properties of Prepared Catalysts

	BET surface area (m^2/g)	relative surface area	relative activity
wet impregnation	127	1.00	1.00
co-deposition (w/o surfactant)	330	2.59	2.17
w/ 10 mM CTAB	528	4.15	3.31
w/ 1 mM HDA	615	4.84	3.78

the supported catalyst at higher vanadium concentrations was due to dissolution of the excess vanadia, with the dissolved vanadium ions continuing to act as catalysts in the solvated state.[37] That is, the increase in activity beyond 21.8 cat. % vanadium would not continue to be observed in a flowing system once the excess vanadium was washed out of the catalyst. (In contrast, none of the co-deposited materials with < 70 cat. % V showed evidence of vanadium leaching.) Therefore, in comparisons of performance, 21.8 cat. % vanadium in the reference catalysts was considered equivalent to 100 cat. % vanadium in the co-deposited materials, that is, both cases representing effectively full vanadium loading of the catalyst surface.

Catalytic Activity of Co-deposited Titanium−Vanadium Oxides. Figure 8 compares the kinetics of the oxidation of lactic acid by hydrogen peroxide in the presence of Ti−V oxide powders of various chemical compositions made via co-deposition without surfactant (Figure 1), with 10 mM CTAB (Figure 2), and with 1 mM HDA (Figure 4) to that of the reference material made via wet impregnation at equivalent values of surface coverage. For a given synthesis technique, the kinetics increased with increasing vanadium loading. This indicates that vanadium is the active catalytic component of the Ti−V materials.

The relative activities of the catalysts decreased in the order HDA > CTAB > co-deposited with no surfactant > reference catalyst (Figure 8). This trend was also reflected (although less than linearly) in the surface areas of the prepared catalysts (Table 3) and in the apparent surface area of the powders as observed with TEM (Figures 1, 2, and 4): HDA yielded a large percentage of very fine filaments, the highest surface area, and the highest catalytic activity; and the CTAB yielded bundles of nanotubes, giving the next highest surface area and catalytic activity. Materials co-deposited without surfactant still showed higher surface area than the impregnated titania support, attributable at least in part to the lack of a high-temperature calcination step in the synthesis of the co-deposited materials. These results show that the micelle strategy was effective at creating nanoscale porosity in Ti−V catalyst compositions, increasing their surface area and their catalytic activity.

The measured surface areas for the materials made using surfactant are lower than expected; for MCM-41 materials, which are also synthesized using a surfactant-micelle technique, the surface area is typically about 1000 m^2/g. This suggests that not all of the present material made using surfactants was mesoporous or that not all of the mesopore surfaces were equally accessible. That is, although the diameter of the nanotubes (∼4 nm) is much larger than the sizes of the lactic acid and pyruvic acid molecules (∼0.5 nm), transport of reactants into, and products out of, the nanotube bundles (Figure 2) and clusters of nanotube filaments (Figure 4), hundreds of nanometers long, may be slower than that on the surface of the materials made without surfactants. Future research can be directed at optimizing the synthesis and handling procedures to further increase the surface area and thus improve the catalytic activity of these materials.

Conclusions

Mixed titanium−vanadium oxides were fabricated using co-deposition from aqueous solutions. As-prepared solids showed a $(Ti,V)O_{2+\delta}$ phase with the anatase structure. Titanium−vanadium oxide was also deposited on micelles of CTAB and HDA, yielding mesoporous solids with pores of 4.1 and 3.7 nm, respectively, as observed using TEM and XRD. The microstructure of solids prepared with CTAB showed a typical mesoporous structure. With HDA, the microstructure showed cactuslike clusters of nanotubes.

The catalytic behavior of these solids was characterized using a vanadium-catalyzed oxidation of lactic acid to pyruvic acid using hydrogen peroxide as regenerating agent. The kinetics was pseudo-first order, with the rate proportional to the vanadium loading in the catalyst. The activity of mesoporous structures (prepared with CTAB) was 3.3 times higher than that of the materials obtained via wet impregnation, while the activity of the cactus structures (prepared with HDA) was 3.8 times higher. The catalytic activity increased with surface area of the powders, but less than linearly, suggesting that not all of the surface area of the mesoporous material was equally accessible for the lactic acid−pyruvic acid reaction.

This work showed that mixed-oxide catalysts, prepared using a simple aqueous synthesis procedure that takes advantage of principles of surface chemistry, exhibited greater performance than that of conventionally prepared materials of comparable compositions. The improved performance is attributed to the existence of nanoscale porosity in the new materials, imparted through the use of surfactant solutions at ∼10 × CMC during synthesis.

Acknowledgment. This paper was based in part on a thesis submitted for the Ph.D. degree in Materials Science and Engineering of J.-J.S., Case Western Reserve University, 2004. This research was supported by the U.S. National Science Foundation through grants DMR 9803851 and DMR 0203655. We acknowledge Prof. Frank Ernst (CWRU) and Dr. Ming Zhang (CWRU) for assistance and advice with the TEM work,

Dr. Lizhi Liu and Dr. Yin Tang (Nanocerox) for help with surface area measurements, and Dr. Yu-Tsai Hsieh (Eternal Chemical), Dr. Kuo-Wei Huang (Brookhaven National Laboratory), Berry Chou (CWRU), Jyun-Hwei Hwang (National Taiwan University), and Chung-Wai Shiau (Ohio State University) for their assistance.

Note Added in Proof. Fu et al. recently reported doping an anatase nanoparticle suspension with vanadium via a solution process. Fu, G.; Vary, P. S.; Lin, C.-T. *J. Phys. Chem. B* **2005**, *109*, 8889−8898.

JA0536365